

DONUT: A Decoder-Only Model for Trajectory Prediction

Markus Knoche¹ Daan de Geus^{1,2} Bastian Leibe¹

¹RWTH Aachen University ²Eindhoven University of Technology

vision.rwth-aachen.de/DONUT

Abstract

Predicting the motion of other agents in a scene is highly relevant for autonomous driving, as it allows a self-driving car to anticipate. Inspired by the success of decoder-only models for language modeling, we propose DONUT, a Decoder-Only Network for Unrolling Trajectories. Different from existing encoder-decoder forecasting models, we encode historical trajectories and predict future trajectories with a single autoregressive model. This allows the model to make iterative predictions in a consistent manner, and ensures that the model is always provided with up-to-date information, enhancing the performance. Furthermore, inspired by multi-token prediction for language modeling, we introduce an ‘overprediction’ strategy that gives the network the auxiliary task of predicting trajectories at longer temporal horizons. This allows the model to better anticipate the future, and further improves the performance. With experiments, we demonstrate that our decoder-only approach outperforms the encoder-decoder baseline, and achieves new state-of-the-art results on the Argoverse 2 single-agent motion forecasting benchmark.

1. Introduction

Motion forecasting is a crucial task for autonomous driving. By predicting the future trajectories of agents in a scene, a self-driving car can anticipate and adjust its behavior. To forecast agents’ motion accurately, a model needs to take into account the geometry of the surrounding road, the presence of other agents, and an agent’s historical behavior. Most recent motion-forecasting works [19, 35, 41, 51, 55], employ a model with two different modules for this purpose (Fig. 1a): (1) an *encoder* that embeds the historical trajectories into a latent space while considering the road layout and agent interactions, and (2) a *decoder* that takes these embeddings and predicts the future trajectories, again taking into account road geometry and agent interactions. While these *encoder-decoder* methods obtain impressive results [19, 51, 55], we posit that a *decoder-only* model is bet-

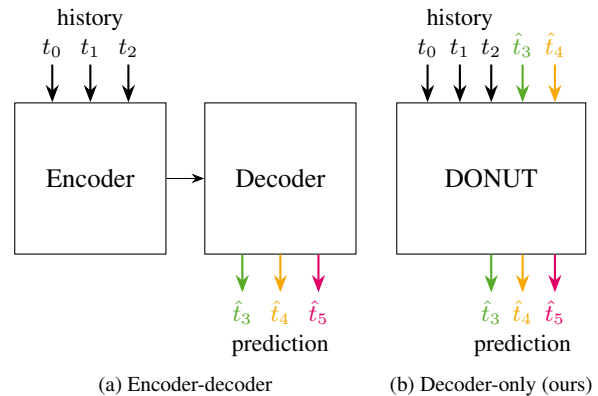


Figure 1. **Encoder-decoder vs. decoder-only methods for motion forecasting.** In contrast to existing works, which use an encoder-decoder architecture, DONUT uses a unified, autoregressive model to process agents’ historical and future trajectories. This allows it to predict trajectories at different timesteps in a consistent manner and receive up-to-date information of relevant scene elements, improving its performance.

ter suited for this task, as it allows us to treat historical and future trajectories in a *unified* manner.

In existing encoder-decoder methods, agents’ future trajectories are predicted by the decoder. Based on the historical embeddings generated by the encoder, the decoder typically predicts the future trajectory either (a) in its entirety, in a single pass [19, 35, 41], or (b) recurrently [34, 37, 55]. Both of these configurations have limitations. When predicting the entire trajectory in a single pass, the network is not adequately aware of the scene elements towards the end of the predicted trajectories. We expect this to negatively impact the accuracy of ‘far-future’ predictions, leading to the use of anchors or goal points in some models to mitigate this [22, 45, 46]. This limitation is addressed in part by using a recurrent method [55], where the decoder predicts future trajectories in an iterative manner, being updated about relevant scene points for each future sub-prediction. However, the feature representation of input data received by this decoder varies between different timesteps, which unneces-

sarily complicates the decoder’s task. Moreover, it receives only the original historical embeddings of other agents as provided by the encoder, which become outdated when predicting ‘far-future’ trajectories, again limiting the ability to make an informed prediction. See Sec. 3.2 for more details.

In this work, we propose a method that overcomes these limitations by treating the historical time steps and future time steps in a unified manner, using a *decoder-only network* (Fig. 1b). We call this the *Decoder-Only Network for Unrolling Trajectories* (DONUT). In DONUT, we use a single network module to process both the historical and the future trajectories in an autoregressive manner. In each step, the model is informed of the scene elements—road geometry and other agents—around the endpoint of the previously predicted trajectory. As such, the network is aware of the relevant scene elements—including other agents’ trajectories—at all times. Furthermore, because of the autoregressive decoder-only formulation, each future trajectory prediction is made based on the embeddings of the trajectories at all previous time steps, generated by the same model. As such, each prediction is made in a consistent manner. We expect that this allows the model to naturally transfer what it learns about historical trajectories to the future, and that it simplifies the task for the model, enabling it to predict future trajectories more accurately.

Our decoder-only approach to future trajectory prediction has similarities with autoregressive Large Language Models (LLMs) [33]. Interestingly, recent works [15] have demonstrated that an LLM’s output quality can be improved by tasking the model with *multi-token prediction*. During training, the LLM additionally predicts tokens that are further in the future, supervised with an auxiliary loss. This stimulates the model to better take into account possible futures during training. Inspired by this finding, we propose to adapt this concept for trajectory forecasting. Concretely, when predicting a future trajectory segment, we let the model not only predict the current segment, but also the next segment. We expect that this *overprediction* strategy enables DONUT to look further into the future when making its predictions, allowing it to better anticipate and predict a more consistent future trajectory. Furthermore, we introduce a refinement module to enhance the initial predictions, which receives updated information to other scene elements at the endpoint of the initially predicted trajectory.

Through experimental evaluation, we find that our decoder-only model outperforms the encoder-decoder baseline, especially on the minFDE metric that considers the accuracy of the forecasted trajectory’s endpoint. Moreover, we find that our overprediction strategy further positively impacts performance. This demonstrates the value of our proposed approach. Compared to existing top-performing methods, DONUT also performs considerably better on the minFDE and brier-minFDE metrics and obtains new state-

of-the-art results on the Argoverse 2 benchmark [47].

In summary, our contributions are as follows:

- We present DONUT, an autoregressive decoder-only model for motion forecasting, which uses the same unified model to process historical and future trajectories.
- We propose the *overprediction* strategy, where a model is asked to predict further into the future to better anticipate different future possibilities.
- With our approach, we achieve state-of-the-art performance on the Argoverse 2 benchmark.

2. Related Work

Motion forecasting. Early motion forecasting models [3, 8, 13, 17, 20, 30, 36, 40] rasterize maps and use convolutional neural networks to extract features about the surroundings. As this results in precision losses, modern approaches follow VectorNet [11] and LaneGCN [21] and directly use vectorized data. Such models are commonly based on graph convolutions [12, 14, 21, 26, 50] or use attention [22, 24, 28, 38, 46, 49, 51, 55] for interaction between scene elements.

After all scene elements are encoded and have interacted with each other in an encoder, many older methods often either use recurrent models [17, 20, 36, 40] or shallow feedforward networks [11, 21, 28, 54] to predict the output trajectories. Recent architectures [14, 29, 38, 51, 55] commonly use attention-based decoders to allow for further interaction between agents, between different modes, and with the road layout information. Some works [6, 41, 53, 55] also incorporate an additional refinement module which enhances the model’s initial predictions. In this work, we diverge from the common encoder-decoder structure, and instead present a decoder-only model, called DONUT. We apply a refinement module after each prediction step to improve the trajectory and combine this with an overprediction strategy.

Many current approaches use an agent-centric coordinate system [38, 40, 46, 52, 54]. A downside of this approach is that all scene elements have to be converted into each agent’s reference frame separately, which comes at an extra cost. An alternative is the use of a single global coordinate system for all agents, which is employed for most raster-based methods but also some more recent models [29]. However, this approach is not position-invariant, meaning that the prediction will change if the whole scene is shifted or rotated. Recently, QCNet [55] proposed a query-centric approach, where each scene element—*i.e.*, road lane or trajectory segment—has its own reference frame, and relative positional encodings are used for interaction between scene elements. We also utilize the query-centric approach in DONUT, as this allows to re-use features from previous timesteps without the need to re-compute them if any position information gets updated.

There are only a few approaches that do not have a distinct agent encoder, like DONUT. Social LSTM [2], one of the oldest deep-learning-based motion forecasting models, uses an LSTM [16] on the full trajectory of pedestrians in a traffic scene. STAR [49] uses an attention-based model which predicts a single timestep using the full history. To predict longer sequences, the prediction is concatenated to the observed history and the full updated trajectory is fed through the model again.

In the related area of motion simulation [27], a few recent models [31, 48, 56] use GPT-style decoder-only models. Different from our approach, these models always predict independent samples from the underlying future distribution. In motion forecasting, we are interested in a fixed number of predictions which should span the possible future as well as possible. As such, these tasks require different approaches. In addition, encoder-decoder approaches trained for motion forecasting can be applied autoregressively for simulation [18, 27, 28]. This has some conceptual similarity to DONUT’s overprediction strategy, as the training horizon extends further than the required horizon during inference. However, these approaches differ as DONUT makes short overpredictions for each individual future token during training, instead of overpredicting the entire future just once, in one pass.

Relation to Large Language Models. The Transformer architecture [44] was initially proposed in the context of language modeling. While this architecture contains an encoder and a decoder, encoder-only [9] or decoder-only [33] models were introduced shortly afterwards. Recently, most well-known large language models [1, 23, 42, 43] use the decoder-only approach, as the causal behavior is a good fit for sequence prediction. As motion forecasting is also a sequence prediction task, this inspired us to apply a decoder-only model. To guide LLMs to better anticipate the future, multi-token prediction [15] tasks a model with predicting tokens for future time steps. In DONUT, we adapt this to the trajectory forecasting task, with ‘overprediction’.

3. Method

We present DONUT, a decoder-only Transformer model for motion forecasting. In this section, we first provide a detailed task definition, then describe the encoder-decoder baseline that we improve upon, and finally present our new method. The overall architecture is visualized in Fig. 2.

3.1. Task definition

Motion forecasting aims to predict the future locations of agents based on their historic behavior and a given scene context. We define the agents’ historic behavior as $\mathbf{X} \in \mathbb{R}^{N \times T_{\text{hist}} \times C}$, where N represents the number of agents in the scene, T_{hist} is the number of observed time steps, and

C is the size of the state of the agent. This state may describe an agents’ position, velocity, motion vector, *etc.* In addition, each agent’s semantic type (*e.g.*, car, pedestrian) is known. Given the historic behavior \mathbf{X} , the task objective is to predict each agent’s position at T_{fut} future time steps. To achieve this, a model is allowed to make K different predictions which are commonly referred to as ‘modes’. In other words, the desired output is a set of K future trajectories for all N agents, given by $\mathbf{Y} \in \mathbb{R}^{N \times K \times T_{\text{fut}} \times C_{\text{pos}}}$, where $C_{\text{pos}} = 2$, as we require each agent’s future (x, y) positions. Additionally, a model should assign a probability to each of the K predictions, so it should output $\mathbf{P} \in \mathbb{R}^{N \times K}$ with $\sum_k \mathbf{P}_{n,k} = 1 \forall n$.

As additional scene context, the road geometry of the scene is available. Each road lane is encoded as a set of polylines, each consisting of a varying number of (x, y) coordinates. Relations between road lanes (*e.g.*, connecting or parallel lanes), and lanes’ semantic categories (*e.g.*, bus lane or part of an intersection) are also known.

3.2. Encoder-decoder baseline

We build our method upon QCNet [55], a top-performing encoder-decoder method for motion prediction. As such, this method serves as our baseline.

Query-centric scene encoding. Both the baseline and our method use a query-centric scene encoding. In this framework, all scene elements—*i.e.*, agents’ trajectories or road lanes—are encoded as tokens that can be processed by a Transformer model [44]. Each token uses its own local reference coordinate system, which means the method is invariant to global positions and orientations. Likewise, instead of using absolute positional encodings, relations between scene elements are encoded in a relative manner. For this, distance, direction, and relative orientation are (1) encoded as Fourier features [39, 44], (2) fed into a multi-layer perceptron (MLP), and (3) added to the respective key and value vectors in the attention operation. If the communicating scene elements belong to different timesteps, the timestep difference is also encoded.

Map encoder. In this baseline, each scene’s road lanes are encoded into a set of tokens through a *map encoder*. Each point on a polyline m is represented by computing Fourier features of the relative distance to the subsequent point and feeding this into an MLP, and adding a learned embedding of the points’ semantic category. Then, an embedding for the polyline’s category attends to these point-level tokens using relative positional encodings, resulting in a single token per polyline that embeds information about all its constituent points. Finally, self-attention enables interaction between different polylines in a certain radius. An embedding encodes the type of the relation within the attention, *e.g.*, whether a polyline is the successor of another or just closeby. This yields the final map tokens $\mathbf{T}_M \in \mathbb{R}^{M \times D}$,

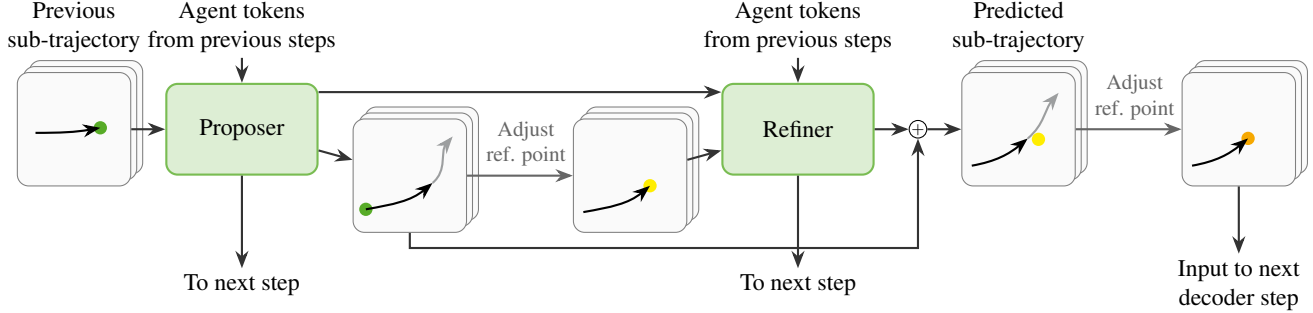


Figure 2. **DONUT architecture overview.** Previously predicted sub-trajectories are fed through a proposer module to make a proposal prediction (\rightarrow) and an overprediction (\rightarrow). The reference point for all relative encodings is then moved to the endpoint of the proposed trajectory (from \bullet to \bullet). Next, the refiner predicts offsets which are added to the proposed trajectories to obtain the final predicted sub-trajectory and overprediction. Before using the predicted sub-trajectory as input to the next decoder step, the reference point is updated to the refined endpoint again (from \bullet to \bullet). For details on the proposer and refiner, see Fig. 3.

where D is the embedding dimension, and M is the number of polylines. In DONUT, we use the same map encoder.

Agent encoder. The baseline further employs an *agent encoder* to represent agents’ historical trajectories as tokens $T_A \in \mathbb{R}^{N \times T_{\text{hist}} \times D}$. Here, for each timestep $t_{\text{hist}} \in \{1, \dots, T_{\text{hist}}\}$, the encoder obtains each motion vector and velocity at each timestep, computes Fourier features, passes them through an MLP, and adds a categorical learned embedding to obtain initial tokens T'_A . Next, each token first interacts with previous tokens of the same agent, then with road tokens T_M , and finally with other agents’ tokens of the same timestep. All interactions are modeled as attention with relative positional encodings. This is repeated twice and yields the updated agent tokens T_A .

Recurrent decoder. To predict future trajectories, the encoder-decoder baseline takes the map tokens T_M and agent tokens T_A , and feeds them through another module, the *recurrent decoder*. In this decoder, learned mode embeddings $E \in \mathbb{R}^{N \times K \times D}$ are introduced, which interact with the agent tokens and map tokens. Concretely, each embedding attends to (1) the historical tokens of the corresponding agent, (2) the map tokens, and (3) the most recent historical token of other agents in the scene. This is repeated $2 \times$ and followed by a self-attention layer across the K different modes. The output embeddings E' are used to predict the trajectory $\hat{Y}'_{\text{dec}} \in \mathbb{R}^{N \times K \times T_{\text{dec}} \times C_{\text{pos}}}$ for the next $T_{\text{dec}} \leq T_{\text{fut}}$ timesteps, for all agents and modes.

This process is repeated until there is a prediction for all T_{fut} timesteps, $\hat{Y}'_{\text{fut}} \in \mathbb{R}^{N \times K \times T_{\text{fut}} \times C_{\text{pos}}}$. In these subsequent iterations, the learned embeddings E are replaced by the decoder’s output embeddings E' of the previous iteration. Note that this introduces inconsistencies, as the decoder either takes (a) a learned embedding or (b) an earlier output embedding as input, and has to learn to handle both cases. We hypothesize that this limits performance, as it complicates the decoder’s task. Moreover, in later iterations, the

historical agent tokens T_A are not updated with the previous predictions. As a result, the agent encoder only provides the decoder with ‘outdated’ information when predicting further into the future. We expect that this harms the accuracy of the baseline’s *far-future* prediction.

Finally, QCNet employs an additional refinement module on the full proposed trajectory \hat{Y}'_{fut} . This module embeds the initial predictions as tokens with a gated recurrent unit (GRU) [5], applies the aforementioned attention operations to the historic agent tokens T_A and map tokens T_M , and outputs an offset to the original predictions. This results in refined trajectories $\hat{Y}_{\text{fut}} \in \mathbb{R}^{N \times K \times T_{\text{fut}} \times C_{\text{pos}}}$.

3.3. DONUT

Our decoder-only network, DONUT, uses the same query-centric formulation as the baseline, but it does not employ an encoder-decoder structure that requires different modules to embed agents’ histories and predict future trajectories. Instead, we propose to use a single, unified decoder to process agents’ trajectories in an autoregressive manner, for both historical and future timesteps. This allows the decoder to use the same procedure to make future predictions at any timestep, avoiding any inconsistencies. Moreover, it ensures that the decoder is always provided with ‘up-to-date’ information about agents’ trajectories, allowing it to make more informed predictions about the far future.

Overall architecture. To process and predict trajectories in an autoregressive manner, we split all agents’ trajectories into sub-trajectories of T_{sub} timesteps. These sub-trajectories are then fed through our decoder-only model. Starting with the predicted sub-trajectories of the previous timestep, $\hat{Y}_{\{-T_{\text{sub}}; 0\}} \in \mathbb{R}^{N \times K \times T_{\text{sub}} \times C_{\text{ph}}}$, our model uses a *proposer* module to predict the sub-trajectories of the next T_{sub} timesteps, $\hat{Y}'_{\{0; T_{\text{sub}}\}} \in \mathbb{R}^{N \times K \times T_{\text{sub}} \times C_{\text{ph}}}$. Furthermore, to enable the network to better anticipate possible futures, we also task it to predict the trajectory for the

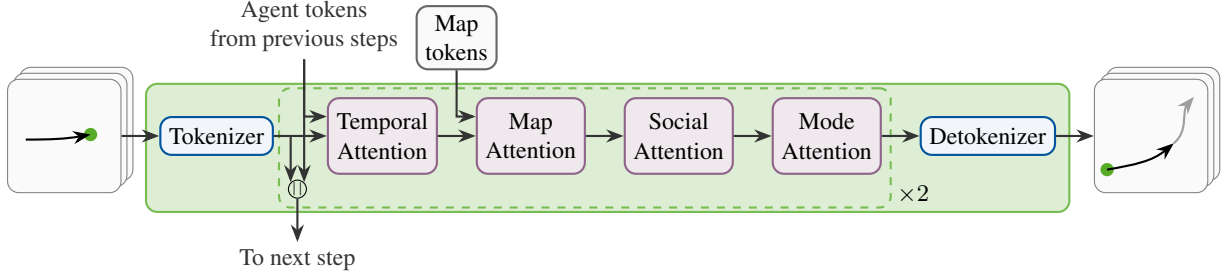


Figure 3. **Proposer architecture.** The input sub-trajectory is first tokenized relative to the reference point (●). Then, the tokens attend to (1) sub-trajectory tokens from previous decoder steps, (2) map tokens, (3) nearby agents, and (4) other modes of the same agent. All attention operations use relative positional encodings based on the current reference point (●). Finally, a detokenizer outputs the next sub-trajectory and an overprediction. The refiner model has the exact same architecture, only the inputs and outputs differ.

T_{sub} -long sub-trajectories that follow the initial predictions $\hat{\mathbf{Y}}'_{\{0;T_{\text{sub}}\}}$. This results in an *overprediction* which we denote by $\hat{\mathbf{Y}}'_{\{T_{\text{sub}};2T_{\text{sub}}\}}^{\text{over}}$. These overpredictions are supervised during training, but discarded during inference. Next, we update the reference point to the endpoint of initial prediction $\hat{\mathbf{Y}}'_{\{0;T_{\text{sub}}\}}$ and recompute the relative positional encodings to other scene elements. These are used by the refinement module together with the tokenized initial predictions and features from the proposer to predict an offset to obtain refined predictions $\hat{\mathbf{Y}}_{\{0;T_{\text{sub}}\}}$ and refined overpredictions $\hat{\mathbf{Y}}_{\{T_{\text{sub}};2T_{\text{sub}}\}}^{\text{over}}$. This process is visualized in Fig. 2.

The output of each decoder step is a set of predicted trajectories $\hat{\mathbf{Y}}_{\{0;T_{\text{sub}}\}}$ and overpredicted trajectories $\hat{\mathbf{Y}}_{\{T_{\text{sub}};2T_{\text{sub}}\}}^{\text{over}}$. The predicted trajectories are then stored and used as an input to the decoder in the next step, where the trajectory for the subsequent T_{sub} timesteps will be predicted. This is continued until all sub-trajectories have been processed and all future trajectories $\hat{\mathbf{Y}} \in \mathbb{R}^{N \times K \times T_{\text{fut}} \times C_{\text{ph}}}$ have been predicted. Besides the position, we also predict each agent’s heading at each time step, so $C_{\text{ph}} = 3$. Our model requires this information to appropriately update the reference coordinate frame.

Proposer and refiner. The proposer and refiner use the same architecture to make their predictions (see Fig. 3). First, the input sub-trajectories are encoded as tokens by the *tokenizer*. For each of the T_{sub} timesteps of a sub-trajectory, this tokenizer extracts the position, heading, motion vector, and velocity with respect to the reference coordinate frame. For this coordinate frame, we use the endpoint of the sub-trajectory. Following our baseline, we compute Fourier features for each timestep separately. To merge the T_{sub} timesteps into a single token, we pass each timestep’s features through an MLP, concatenate the T_{sub} resulting embeddings, and process them by another MLP, finally outputting a token for each sub-trajectory. This is combined with an embedding of the agent type. We denote these tokens as $\mathbf{T}_{\text{sub}} \in \mathbb{R}^{N \times K \times D}$.

In the remainder of the module, these tokens are subjected to various types of attention. (1) *Temporal self-attention*: Each token $\mathbf{T}_{\text{sub}} \in \mathbb{R}^{N \times K \times D}$ attends to all historical sub-trajectory tokens of the same agent. These historical tokens are retrieved from the proposer and refiner modules from the previous decoder steps to keep them up-to-date, as visualized in Fig. 3. (2) *Map attention*: The tokens cross-attend to the tokens from road lanes within a radius r of the reference point. To obtain these tokens, we use the same map encoder as the baseline. (3) *Social attention*: To make agents aware of the behavior of other agents within radius r that have the same mode. (4) *Mode attention*: Finally, to ensure that there is interaction between the K different modes, tokens self-attend to tokens that have different modes but belong to the same agent. This whole process is conducted twice in both proposer and refiner.

After this factorized attention, the tokens are decoded with a *detokenizer* to predict the next sub-trajectories and generate the overpredictions using an MLP. An additional MLP outputs a logit for each mode of each agent at the final timestep of the refiner, which we use to compute the mode probabilities.

To initialize the model with the historic tokens $\mathbf{X} \in \mathbb{R}^{N \times T_{\text{hist}} \times C}$, we feed historic trajectories into both proposer and refiner. These historic trajectories can be processed in parallel. As the only purpose is to produce historic agent tokens for the temporal attention, we can discard the predictions. We run this in a unimodal setting, *i.e.*, $K = 1$. After the last timestep of the historic trajectory, we duplicate the tokens along the mode dimension. From this point on, the model is multimodal. To allow the models to distinguish different modes, we add a mode embedding for each mode within the mode attention. As the modes diverge over time, we also make the mode attention aware of the timestep since starting the multimodal predictions, using a time embedding.

Training. During training, we supervise the predicted and overpredicted trajectories of the T_{fut} future timesteps. Following HiVT [54] and QCNet [55], the positions that are predicted as part of $\hat{\mathbf{Y}} \in \mathbb{R}^{N \times K \times T_{\text{fut}} \times C_{\text{ph}}}$ are parametrized using a mixture of Laplace distributions. For an agent $n \in \{1, \dots, N\}$, for each timestep $t \in \{1, \dots, T_{\text{fut}}\}$, and for each mode $k \in \{1, \dots, K\}$, the model outputs the Laplace parameters location $\mu_{n,k,t}^{\text{pos}}$ and scale $b_{n,k,t}^{\text{pos}}$, together with mode probabilities $P_{n,k}$. This results in a likelihood

$$p(\hat{\mathbf{Y}}_n^{\text{pos}}) = \sum_{k=1}^K P_{n,k} \prod_{t=1}^{T_{\text{fut}}} \text{Laplace}(\hat{\mathbf{Y}}_{n,t}^{\text{pos}} | \mu_{n,k,t}^{\text{pos}}, b_{n,k,t}^{\text{pos}}). \quad (1)$$

Additionally, to update the reference point at each decoder step, DONUT requires the agent’s heading. For this, we use the von-Mises distribution. Specifically, the model outputs location $\mu_{n,k,t}^{\text{hd}}$ and concentration $\kappa_{n,k,t}^{\text{hd}}$, and the likelihood is given by

$$p(\hat{\mathbf{Y}}_n^{\text{hd}}) = \sum_{k=1}^K P_{n,k} \prod_{t=1}^{T_{\text{fut}}} \text{vonMises}(\hat{\mathbf{Y}}_{n,t}^{\text{hd}} | \mu_{n,k,t}^{\text{hd}}, \kappa_{n,k,t}^{\text{hd}}). \quad (2)$$

Following QCNet, we optimize the parameters of the Laplace and von-Mises distributions ($\mu_{n,k,t}^{\text{pos}}, b_{n,k,t}^{\text{pos}}, \mu_{n,k,t}^{\text{hd}}, \kappa_{n,k,t}^{\text{hd}}$) only for the mode where the proposed trajectory has the smallest endpoint distance to the ground truth. The loss is applied for proposed and refined trajectories independently, for both main predictions and overpredictions, and gradients are stopped after the output of the proposed trajectory. We apply the same procedure for the overpredictions. The mixture components $P_{n,k}$ are optimized using the joint negative log-likelihood of Eq. (1) and Eq. (2). All losses are weighed equally.

4. Experiments

4.1. Experimental setup

Datasets. We assess the effectiveness of our model on the competitive Argoverse 2 single-agent forecasting benchmark [47]. We train on the *train* set, which consists of 200k scenes, and evaluate on the *val* set and the hidden *test* set, each containing 25k scenes. Each scene is 11 s long, sampled at 10 Hz. Of these 11 s, the model takes the trajectory of the first 5 s as input and predicts $K = 6$ trajectories for the last 6 s. In other words, there are $T_{\text{hist}} = 50$ historical time steps and $T_{\text{fut}} = 60$ future time steps.

Metrics. We use the benchmark’s default metrics for evaluation [47]. The *minimum final displacement error* (minFDE_K) computes the L2 distance between the endpoint of the ground-truth trajectory and the endpoint of the ‘best’ predicted trajectory, across the K predicted modes. Here, a predicted trajectory is the ‘best’ if it has the lowest endpoint error. Similarly, the *minimum average displacement error* (minADE_K) computes the average L2 distance be-

tween the ground-truth trajectory and the best predicted trajectory. The *miss rate* (MR) reflects the percentage of scenarios for which the endpoints of none of the predicted trajectories are within 2.0 m of the ground truth’s endpoint. Finally, the main metric for the benchmark, the *brier-minFDE* is defined as

$$\text{b-minFDE}_K = (1 - \pi)^2 + \text{minFDE}_K, \quad (3)$$

where π is the predicted probability for the best predicted trajectory. This metric captures the ability to both predict an accurate future trajectory and assign a high probability to the trajectory that best matches the ground truth, which is relevant in real-world scenarios. The default setting for our experiments is $K = 6$, but we also report $K = 1$ for test set evaluations, which picks the mode with the highest probability.

Implementation details. We implement DONUT within the publicly released code repository of QCNet [55]. In our decoder-only model, we use sub-trajectories of $T_{\text{sub}} = 10$ time steps, *i.e.*, one second. Each token can interact with other agents and map elements that are within $r = 50$ m of its reference point. DONUT is trained using the AdamW optimizer [25], with a weight decay of 10^{-4} , an initial learning rate of $5 \cdot 10^{-4}$, and a cosine learning rate decay schedule. We train for 60 epochs with batches of 8 scenes per GPU across 4 H100 GPUs, and we accumulate gradients to obtain a virtual batch size of 64. We use an embedding dimension of $D = 128$ and a dropout rate of 10%.

Encoder-decoder baseline. As described in Sec. 3.2, we use QCNet [55] as our encoder-decoder baseline. For this model, we use the publicly released code and weights.

4.2. Main results

First, we assess the impact of switching from the encoder-decoder approach to our decoder-only setup. The results in Tab. 1 demonstrate that switching to our decoder-only setup without using *overprediction* or *refinement* boosts the performance across the main b-minFDE_6 metric, the minFDE_6 , and the MR_6 . This demonstrates that using the same unified model structure for both historical and future trajectories allows the model to make more accurate predictions, as hypothesized. On the minADE_6 metric, however, the encoder-decoder baseline performs slightly better. We attribute this to the fact that the baseline’s agent encoder generates a single token per time step, giving it a higher granularity.

When also training our model to *overpredict* future trajectories, the performance slightly improves further, especially for minADE_6 . The improvements obtained by using overprediction are much larger, though, when also using our *refinement* module. The use of the refinement module alone slightly lowers performance, except for b-minFDE_6 . Training was less stable in this setting. We hypothesize that overprediction helps DONUT to find a better optimum by forc-

Decoder-only	Overpredict	Refine	b-minFDE₆↓	minFDE ₆ ↓	minADE ₆ ↓	MR ₆ ↓
✗	N/A	N/A	1.874	1.253	0.720	0.157
✓	✗	✗	1.838	1.198	0.745	0.145
✓	✓	✗	1.838	1.193	0.728	0.146
✓	✗	✓	1.835	1.218	0.751	0.150
✓	✓	✓	1.807	1.176	0.722	0.144

Table 1. **Ablation study.** We demonstrate the effectiveness of (1) using our *decoder-only* approach instead the encoder-decoder baseline [55], (2) the *overprediction* objective, and (3) the *refinement* module. Evaluation on the Argoverse2 *val* set [47].

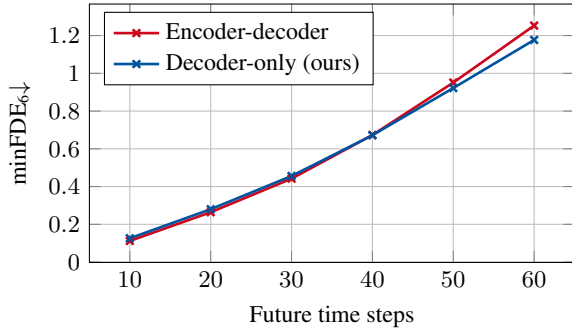


Figure 4. **Performance at different prediction horizons.** Compared to the encoder-decoder baseline, our decoder-only approach makes more accurate predictions at longer prediction horizons.

ing it to consider longer temporal horizons, which stabilizes training and unlocks the refiner’s full potential. We note that the full model trains remarkably stable, with a standard error of 0.003 m on the minFDE across 3 training runs.

To further assess the impact of the decoder-only model, we examine the final displacement error across various prediction lengths ranging from 10 to 60 time steps (Fig. 4). The results indicate that the decoder-only approach yields significantly improved forecasts for longer prediction intervals. This finding supports our hypothesis that (a) having access to up-to-date previous trajectories in our decoder-only model is particularly beneficial for longer prediction horizons, and (b) that overprediction enables the model to better anticipate the far future.

4.3. Comparison to state of the art

To assess the effectiveness of DONUT compared to existing models, we submit it to the Argoverse 2 *test* leaderboard and report the results in Tab. 2. The results demonstrate that DONUT outperforms all other non-ensemble models on the main metric, the b-minFDE₆, by considerable margins. As such, it obtains new state-of-the-art results. This demonstrates that DONUT can accurately predict the endpoint of the future trajectory with one of its 6 predictions, and can assign a high probability to the predicted trajectory that is closest to the ground truth. On other metrics, we also achieve new state-of-the-art results or obtain highly competitive scores which shows the strength of our approach.

DONUT only slightly underperforms DeMo [51] on the minADE₁ and minFDE₁ metrics, but these unimodal metrics are not suitable for multimodal prediction. An optimal model would always predict the *mean* of the future distribution and assign it the highest probability, which often is very unlikely in reality. To clarify, consider an example where a car approaches an intersection where turning left and turning right is equally likely. Here, the optimal prediction for minADE₁ and minFDE₁ would be to stop in the middle of the intersection. In contrast, DONUT does achieve state-of-the-art results on the MR₁ metric, which would penalize a mean prediction, as stopping in the middle of the road will most likely not be close to the actual future.

4.4. Qualitative results

We present a few selected qualitative examples contrasting the encoder-decoder baseline with DONUT in Fig. 5. The left example shows the car approaching a normal intersection. While DONUT manages to correctly predict the right turn with most of its modes, QCNet turns too late and heads into oncoming traffic. The middle example visualizes a scenario where the agent has to drive close to the middle of the road as cars are parked on the side. QCNet predicts that the car would go back to the middle of its lane far too early, where it would hit the parked cars, while DONUT manages to keep a safe distance. Both examples showcase the effectiveness of our regular reference point updates during unrolling the future, allowing the model to better take into account scene elements at future timesteps.

The third example depicts a particularly complex intersection with many crossing lanes and uncommon polygon shapes. Our decoder-only approach predicts most modes turning left, following the trajectory of the previous car. A single trajectory also drives straight and matches the ground truth observation really well, while another prediction stops before the intersection and the last one behaves weirdly. In contrast, the encoder-decoder baseline has huge issues with this scene. The two modes going straight leave the street at their endpoint. A third mode turns right in the middle of the intersection and heads into the oncoming traffic. The other three modes turn left, where one overshoots the curve and another shows a strong discontinuity where QCNet splits the prediction into the recurrent parts. Further examples,

Method	b-minFDE₆↓	minFDE ₆ ↓	minADE ₆ ↓	MR ₆ ↓	minFDE ₁ ↓	minADE ₁ ↓	MR ₁ ↓
THOMAS [14]	2.16	1.51	0.88	0.20	4.71	1.95	0.64
Forecast-MAE [4]	2.03	1.39	0.71	0.17	4.35	1.74	0.61
GoRela [7]	2.01	1.48	0.76	0.22	4.62	1.82	0.66
HeteroGCN [12]	2.00	1.37	0.73	0.18	4.53	1.79	0.59
MTR [38]	1.98	1.44	0.73	0.15	4.39	1.74	0.58
GANet [45]	1.96	1.34	0.72	0.17	4.48	1.77	0.59
DySeT [32]	1.93	1.28	0.67	0.16	4.41	1.76	0.61
QCNet [55]	1.91	1.29	0.65	0.16	4.30	1.69	0.59
ProphNet [46]	1.88	1.32	0.66	0.18	4.77	1.76	0.61
SmartRefine [53]	1.86	1.23	<u>0.63</u>	0.15	4.17	<u>1.65</u>	0.58
DeMo [51]	<u>1.84</u>	<u>1.17</u>	0.61	0.13	3.74	1.49	<u>0.55</u>
MacFormer* [10]	1.91	1.38	0.70	0.19	4.69	1.84	0.61
HeteroGCN* [12]	1.90	1.34	0.69	0.18	4.40	1.72	0.59
QCNet* [55]	1.78	1.19	0.62	0.14	3.96	1.56	0.55
SEPT* [19]	1.74	1.15	0.61	0.14	3.70	1.48	0.54
DeMo* [51]	1.73	1.11	0.60	0.12	3.70	1.49	0.55
DONUT (ours)	1.79	1.16	<u>0.63</u>	<u>0.14</u>	<u>4.06</u>	1.66	0.54

Table 2. **Comparison to state of the art.** We compare to published methods on the *test* set of the Argoverse 2 leaderboard [47], and demonstrate that DONUT achieves state-of-the-art performance on the main b-minFDE₆ metric. * Denotes the use of model ensembling.

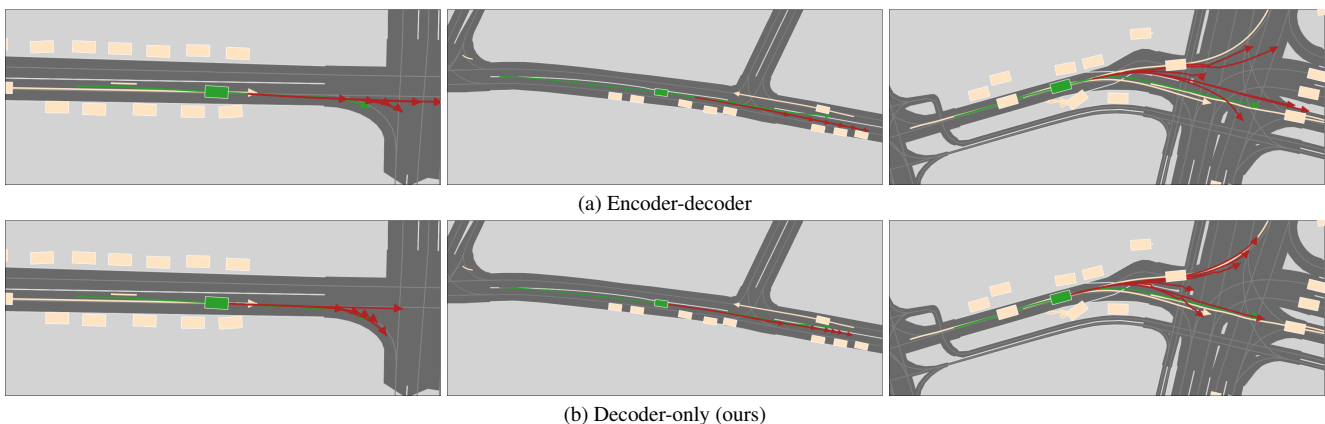


Figure 5. **Qualitative results.** Green trajectories (\rightarrow) show the ground-truth historical and future trajectory of the agent of interest, red trajectories (\rightarrow) visualize the $K = 6$ future predictions. Boxes show the location of the agents at the start of the predicted trajectory. Overall, we observe that DONUT predicts more accurate trajectories than the encoder-decoder baseline.

including visualizations of our ablated models, are in the supplemental material.

5. Conclusion

In this work, we introduce DONUT, an autoregressive decoder-only model for motion forecasting. By processing historical and future trajectories with a unified model, DONUT makes predictions in a consistent manner and is regularly provided with up-to-date information, unlike existing encoder-decoder methods. Furthermore, by employing an innovative overprediction strategy which guides the model to better anticipate the future, DONUT achieves state-of-the-art results on the Argoverse 2 single-agent motion forecasting benchmark for non-ensemble methods.

Our experiments highlight the advantages of the decoder-only paradigm, especially for complex, longer-term predictions. As such, we expect that this approach will generalize well to more complex forecasting scenarios, and we encourage future work in this direction.

Acknowledgments. This work was partially funded by the BMBF project 6GEM (16KISK036K). The authors gratefully acknowledge the Gauss Centre for Supercomputing e.V. (www.gauss-centre.eu) for funding this project by providing computing time on the GCS Supercomputer JUWELS at Jülich Supercomputing Centre (JSC). Further computational resources were provided by the German AI Service Center WestAI under project rwth1815 and by RWTH Aachen University under project rwth1825.

References

- [1] Josh Achiam, Steven Adler, Sandhini Agarwal, Lama Ahmad, Ilge Akkaya, Florencia Leoni Aleman, Diogo Almeida, Janko Altenschmidt, Sam Altman, Shyamal Anadkat, et al. GPT-4 Technical Report. *arXiv preprint arXiv:2303.08774*, 2023. 3
- [2] Alexandre Alahi, Kratharth Goel, Vignesh Ramanathan, Alexandre Robicquet, Li Fei-Fei, and Silvio Savarese. Social Istm: Human trajectory prediction in crowded spaces. In *CVPR*, 2016. 3
- [3] Yuning Chai, Benjamin Sapp, Mayank Bansal, and Dragomir Anguelov. MultiPath: Multiple Probabilistic Anchor Trajectory Hypotheses for Behavior Prediction. In *CoRL*, 2020. 2
- [4] Jie Cheng, Xiaodong Mei, and Ming Liu. Forecast-MAE: Self-supervised Pre-training for Motion Forecasting with Masked Autoencoders. In *ICCV*, 2023. 8
- [5] Kyunghyun Cho, Bart van Merriënboer, Çağlar Gülçehre, Dzmitry Bahdanau, Fethi Bougares, Holger Schwenk, and Yoshua Bengio. Learning Phrase Representations using RNN Encoder–Decoder for Statistical Machine Translation. In *EMNLP*, 2014. 4
- [6] Sehwan Choi, Jungho Kim, Junyong Yun, and Jun Won Choi. R-Pred: Two-Stage Motion Prediction Via Tube-Query Attention-Based Trajectory Refinement. In *ICCV*, 2023. 2
- [7] Alexander Cui, Sergio Casas, Kelvin Wong, Simon Suo, and Raquel Urtasun. GoRela: Go Relative for Viewpoint-Invariant Motion Forecasting. In *ICRA*, 2023. 8
- [8] Henggang Cui, Vladan Radosavljevic, Fang-Chieh Chou, Tsung-Han Lin, Thi Nguyen, Tzu-Kuo Huang, Jeff Schneider, and Nemanja Djuric. Multimodal Trajectory Predictions for Autonomous Driving using Deep Convolutional Networks. In *ICRA*, 2019. 2
- [9] Jacob Devlin, Ming-Wei Chang, Kenton Lee, and Kristina Toutanova. BERT: Pre-training of Deep Bidirectional Transformers for Language Understanding. In *Proceedings of the 2019 conference of the North American chapter of the association for computational linguistics: human language technologies*, 2019. 3
- [10] Chen Feng, Hangning Zhou, Huadong Lin, Zhigang Zhang, Ziyao Xu, Chi Zhang, Boyu Zhou, and Shaojie Shen. MacFormer: Map-Agent Coupled Transformer for Real-Time and Robust Trajectory Prediction. *IEEE RA-L*, 2023. 8
- [11] Jiyang Gao, Chen Sun, Hang Zhao, Yi Shen, Dragomir Anguelov, Congcong Li, and Cordelia Schmid. VectorNet: Encoding HD Maps and Agent Dynamics from Vectorized Representation. In *CVPR*, 2020. 2
- [12] Xing Gao, Xiaogang Jia, Yikang Li, and Hongkai Xiong. Dynamic Scenario Representation Learning for Motion Forecasting With Heterogeneous Graph Convolutional Recurrent Networks. *IEEE RA-L*, 8(5), 2023. 2, 8
- [13] Thomas Gilles, Stefano Sabatini, Dzmitry Tsishkou, Bogdan Stanculescu, and Fabien Moutarde. HOME: Heatmap Output for future Motion Estimation. In *IEEE ITSC*, 2021. 2
- [14] Thomas Gilles, Stefano Sabatini, Dzmitry Tsishkou, Bogdan Stanculescu, and Fabien Moutarde. THOMAS: Trajectory Heatmap Output with learned Multi-Agent Sampling. In *ICLR*, 2022. 2, 8
- [15] Fabian Gloeckle, Badr Youbi Idrissi, Baptiste Roziere, David Lopez-Paz, and Gabriel Synnaeve. Better & Faster Large Language Models via Multi-token Prediction. In *ICML*, 2024. 2, 3
- [16] Sepp Hochreiter and Jürgen Schmidhuber. Long Short-term Memory. *Neural computation*, 1997. 3
- [17] Joey Hong, Benjamin Sapp, and James Philbin. Rules of the Road: Predicting Driving Behavior with a Convolutional Model of Semantic Interactions. In *CVPR*, 2019. 2
- [18] Max Jiang, Yijing Bai, Andre Cornman, Christopher Davis, Xiukun Huang, Hong Jeon, Sakshum Kulshrestha, John Lambert, Shuangyu Li, Xuanyu Zhou, et al. SceneDiffuser: Efficient and Controllable Driving Simulation Initialization and Rollout. In *NeurIPS*, 2024. 3
- [19] Zhiqian Lan, Yuxuan Jiang, Yao Mu, Chen Chen, and Shengbo Eben Li. SEPT: Towards Efficient Scene Representation Learning for Motion Prediction. In *ICLR*, 2024. 1, 8
- [20] Namhoon Lee, Wongun Choi, Paul Vernaza, Christopher B Choy, Philip HS Torr, and Manmohan Chandraker. Desire: Distant future prediction in dynamic scenes with interacting agents. In *CVPR*, 2017. 2
- [21] Ming Liang, Bin Yang, Rui Hu, Yun Chen, Renjie Liao, Song Feng, and Raquel Urtasun. Learning Lane Graph Representations for Motion Forecasting. In *ECCV*, 2020. 2
- [22] Longzhong Lin, Xuewu Lin, Tianwei Lin, Lichao Huang, Rong Xiong, and Yue Wang. EDA: Evolving and Distinct Anchors for Multimodal Motion Prediction. In *AAAI*, 2024. 1, 2
- [23] Aixin Liu, Bei Feng, Bing Xue, Bingxuan Wang, Bochao Wu, Chengda Lu, Chenggang Zhao, Chengqi Deng, Chenyu Zhang, Chong Ruan, et al. DeepSeek-V3 Technical Report. *arXiv preprint arXiv:2412.19437*, 2024. 3
- [24] Yicheng Liu, Jinghui Zhang, Liangji Fang, Qinhong Jiang, and Bolei Zhou. Multimodal Motion Prediction with Stacked Transformers. In *CVPR*, 2021. 2
- [25] Ilya Loshchilov and Frank Hutter. Decoupled weight decay regularization. In *ICLR*, 2017. 6
- [26] Abdullhah Mohamed, Kun Qian, Mohamed Elhoseiny, and Christian Claudel. Social-STGCNN: A Social Spatio-Temporal Graph Convolutional Neural Network for Human Trajectory Prediction. In *CVPR*, 2020. 2
- [27] Nico Montali, John Lambert, Paul Mouglin, Alex Kuefler, Nicholas Rhinehart, Michelle Li, Cole Gulino, Tristan Emrich, Zoey Yang, Shimon Whiteson, et al. The Waymo Open Sim Agents Challenge. In *NeurIPS*, 2023. 3
- [28] Nigamaa Nayakanti, Rami Al-Rfou, Aurick Zhou, Kratharth Goel, Khaled S Refaat, and Benjamin Sapp. Wayformer: Motion Forecasting via Simple & Efficient Attention Networks. In *ICRA*, 2023. 2, 3
- [29] Jiquan Ngiam, Benjamin Caine, Vijay Vasudevan, Zhengdong Zhang, Hao-Tien Lewis Chiang, Jeffrey Ling, Rebecca Roelofs, Alex Bewley, Chenxi Liu, Ashish Venugopal, et al. Scene transformer: A unified architecture for predicting multiple agent trajectories. In *ICLR*, 2022. 2

- [30] Tung Phan-Minh, Elena Corina Grigore, Freddy A Boulton, Oscar Beijbom, and Eric M Wolff. CoverNet: Multimodal Behavior Prediction using Trajectory Sets. In *CVPR*, 2020. 2
- [31] Jonah Philion, Xue Bin Peng, and Sanja Fidler. Trajenglish: Traffic Modeling as Next-Token Prediction. In *ICLR*, 2024. 3
- [32] Mozghan Pourkeshavarz, Junrui Zhang, and Amir Rasouli. DySeT: A Dynamic Masked Self-distillation Approach for Robust Trajectory Prediction. In *ECCV*. Springer, 2024. 8
- [33] Alec Radford, Karthik Narasimhan, Tim Salimans, Ilya Sutskever, et al. Improving Language Understanding by Generative Pre-Training. 2018. 2, 3
- [34] Luke Rowe, Martin Ethier, Eli-Henry Dykhne, and Krzysztof Czarnecki. FJMP: Factorized Joint Multi-Agent Motion Prediction over Learned Directed Acyclic Interaction Graphs. In *CVPR*, 2023. 1
- [35] Hongzhi Ruan, Haibao Yu, Wenxian Yang, Siqi Fan, and Zaiqing Nie. Learning Cooperative Trajectory Representations for Motion Forecasting. In *NeurIPS*, 2024. 1
- [36] Tim Salzman, Boris Ivanovic, Punarjay Chakravarty, and Marco Pavone. Trajectron++: Dynamically-feasible trajectory forecasting with heterogeneous data. In *ECCV*, 2020. 2
- [37] Ari Seff, Brian Cera, Dian Chen, Mason Ng, Aurick Zhou, Nigamaa Nayakanti, Khaled S Refaat, Rami Al-Rfou, and Benjamin Sapp. MotionLM: Multi-Agent Motion Forecasting as Language Modeling. In *ICCV*, 2023. 1
- [38] Shaoshuai Shi, Li Jiang, Dengxin Dai, and Bernt Schiele. Motion Transformer with Global Intention Localization and Local Movement Refinement. In *NeurIPS*, 2022. 2, 8
- [39] Matthew Tancik, Pratul Srinivasan, Ben Mildenhall, Sara Fridovich-Keil, Nithin Raghavan, Utkarsh Singhal, Ravi Ramamoorthi, Jonathan Barron, and Ren Ng. Fourier features let networks learn high frequency functions in low dimensional domains. In *NeurIPS*, 2020. 3
- [40] Charlie Tang and Russ R Salakhutdinov. Multiple Futures Prediction. In *NeurIPS*, 2019. 2
- [41] Xiaolong Tang, Meina Kan, Shiguang Shan, Zhilong Ji, Jinfeng Bai, and Xilin Chen. HPNet: Dynamic Trajectory Forecasting with Historical Prediction Attention. In *CVPR*, 2024. 1, 2
- [42] Gemini Team, Rohan Anil, Sebastian Borgeaud, Jean-Baptiste Alayrac, Jiahui Yu, Radu Soricut, Johan Schalkwyk, Andrew M Dai, Anja Hauth, Katie Millican, et al. Gemini: A Family of Highly Capable Multimodal Models. *arXiv preprint arXiv:2312.11805*, 2023. 3
- [43] Hugo Touvron, Louis Martin, Kevin Stone, Peter Albert, Amjad Almahairi, Yasmine Babaei, Nikolay Bashlykov, Soumya Batra, Prajjwal Bhargava, Shruti Bhosale, et al. Llama 2: Open Foundation and Fine-Tuned Chat Models. *arXiv preprint arXiv:2307.09288*, 2023. 3
- [44] Ashish Vaswani, Noam Shazeer, Niki Parmar, Jakob Uszkoreit, Llion Jones, Aidan N Gomez, Łukasz Kaiser, and Illia Polosukhin. Attention is all you need. In *NeurIPS*, 2017. 3
- [45] Mingkun Wang, Xinge Zhu, Changqian Yu, Wei Li, Yuexin Ma, Ruochun Jin, Xiaoguang Ren, Dongchun Ren, Mingxu Wang, and Wenjing Yang. GANet: Goal Area Network for Motion Forecasting. In *ICRA*, 2023. 1, 8
- [46] Xishun Wang, Tong Su, Fang Da, and Xiaodong Yang. ProphNet: Efficient Agent-Centric Motion Forecasting With Anchor-Informed Proposals. In *CVPR*, 2023. 1, 2, 8
- [47] Benjamin Wilson, William Qi, Tanmay Agarwal, John Lambert, Jagjeet Singh, Siddhesh Khandelwal, Bowen Pan, Ratnesh Kumar, Andrew Hartnett, Jhony Kaesemodel Pontes, Deva Ramanan, Peter Carr, and James Hays. Argoverse 2: Next Generation Datasets for Self-Driving Perception and Forecasting. In *NeurIPS Datasets and Benchmarks*, 2021. 2, 6, 7, 8
- [48] Wei Wu, Xiaoxin Feng, Ziyang Gao, and Yuheng Kan. SMART: Scalable Multi-agent Real-time Motion Generation via Next-token Prediction. In *NeurIPS*, 2024. 3
- [49] Cunjun Yu, Xiao Ma, Jiawei Ren, Haiyu Zhao, and Shuai Yi. Spatio-Temporal Graph Transformer Networks for Pedestrian Trajectory Prediction. In *ECCV*, 2020. 2, 3
- [50] Wenyuan Zeng, Ming Liang, Renjie Liao, and Raquel Urtasun. Lanercnn: Distributed representations for graph-centric motion forecasting. In *IROS*, 2021. 2
- [51] Bozhou Zhang, Nan Song, and Li Zhang. DeMo: Decoupling Motion Forecasting into Directional Intentions and Dynamic States. In *NeurIPS*, 2024. 1, 2, 7, 8
- [52] Hang Zhao, Jiyang Gao, Tian Lan, Chen Sun, Ben Sapp, Balakrishnan Varadarajan, Yue Shen, Yi Shen, Yuning Chai, Cordelia Schmid, et al. TNT: Target-driveN Trajectory Prediction. In *CoRL*, 2021. 2
- [53] Yang Zhou, Hao Shao, Letian Wang, Steven L. Waslander, Hongsheng Li, and Yu Liu. SmartRefine: A Scenario-Adaptive Refinement Framework for Efficient Motion Prediction. In *CVPR*, 2024. 2, 8
- [54] Zikang Zhou, Luyao Ye, Jianping Wang, Kui Wu, and Kejie Lu. HiVT: Hierarchical Vector Transformer for Multi-Agent Motion Prediction. In *CVPR*, 2022. 2, 6
- [55] Zikang Zhou, Jianping Wang, Yung-Hui Li, and Yu-Kai Huang. Query-Centric Trajectory Prediction. In *CVPR*, 2023. 1, 2, 3, 6, 7, 8
- [56] Zikang Zhou, HU Haibo, Xinhong Chen, Jianping Wang, Nan Guan, Kui Wu, Yung-Hui Li, Yu-Kai Huang, and Chun Jason Xue. Behaviorgpt: Smart agent simulation for autonomous driving with next-patch prediction. In *NeurIPS*, 2024. 3

DONUT: A Decoder-Only Model for Trajectory Prediction

Supplementary Material

A. LineAttention

In preliminary experiments, we found it beneficial to give the agent better access to road elements. Our baseline, QC-Net, uses the beginning of a road polyline as the reference point for relative positional encodings. In addition to this, we add an encoding for relative information between the agent and its closest point on each map polyline, which we call *LineAttention*. However, for the final model, this procedure only had a tiny effect, decreasing minFDE from 1.181 to 1.176.

B. Efficiency Analysis

We measure inference time and show the number of parameters in Tab. 3. Due to the temporal unrolling, switching from the baseline to decoder-only almost triples the inference time. The refinement layer roughly doubles the number of successive operations and thus also the inference time. Training times behave similarly. Overprediction has negligible impact on efficiency and is dropped for inference. Note, however, that we did not focus on optimizing the code for efficiency, but instead on improving the prediction accuracy.

DONUT	Ref.	Inference time (ms)	Num. parameters
✗	N/A	23.7	7.7M
✓	✗	65.7	5.2M
✓	✓	129.0	9.0M

Table 3. **Efficiency analysis** on an Nvidia RTX 4090 GPU.

C. Difficult Scenes

To assess DONUT on more challenging scenarios, we evaluate it on Argoverse 2 trajectories with a ground-truth future turn of at least 45° in Tab. 4. The relative improvement with respect to the encoder-decoder baseline becomes notably larger than on the full dataset (14.6% vs. 6.1% minFDE), showing that DONUT’s periodic updates are especially helpful in complex situations.

DONUT	Overp.	Ref.	b-minFDE	minFDE	minADE	MR
✗	N/A	N/A	3.008	2.394	1.176	0.362
✓	✗	✗	2.766	2.129	1.147	0.308
✓	✓	✗	2.725	2.078	1.109	0.308
✓	✗	✓	2.757	2.148	1.160	0.329
✓	✓	✓	2.672	2.043	1.092	0.295

Table 4. **Results on Argoverse 2, only considering turns $> 45^\circ$.**

D. Tokenizer Details

In Fig. 6 we visualize our tokenizer’s architecture in detail. The 8-dimensional features for each timestep consist of position and heading relative to the reference point, motion vectors, angular motion, velocity and the difference of the heading and the motion vector direction. Type embeddings describe the object types (*e.g.*, car, bus, pedestrian) present in Argoverse 2.

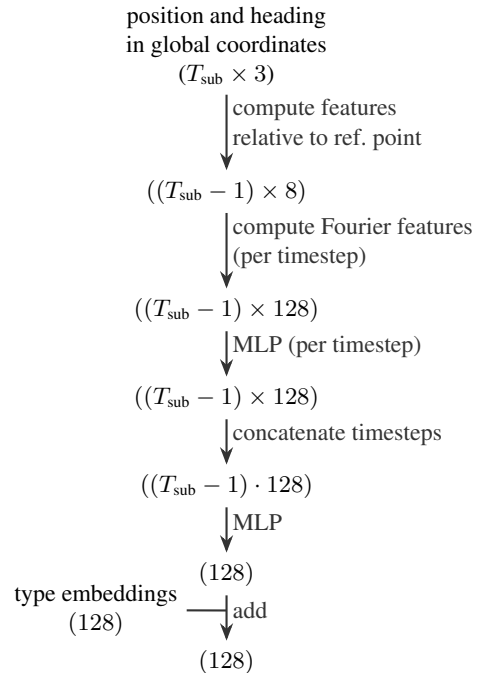


Figure 6. **Detailed tokenizer architecture.**

E. Failure Cases

We manually examined 100 scenes with a minFDE > 5 m. Most errors are caused by predictions being too slow (27%) or too fast (19%), or missing a turn (19%). Additionally, 27% had rare ground-truth events, *e.g.*, vehicles moving off the road or maneuvering illegally. We visualize a few scenes in Fig. 7.

F. Additional Qualitative Results

We provide additional non-cherry-picked qualitative results in Figs. 8 to 23.

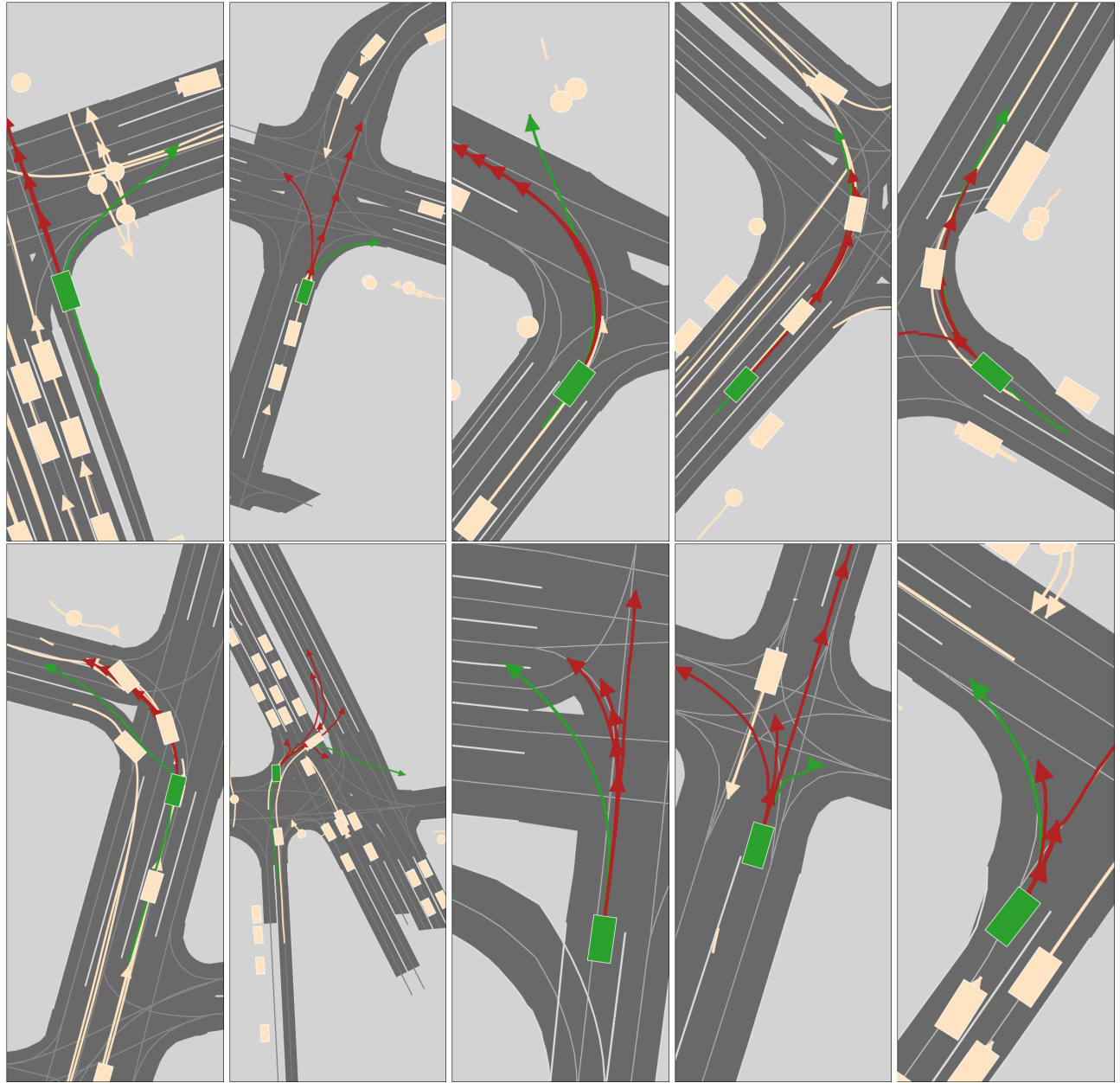
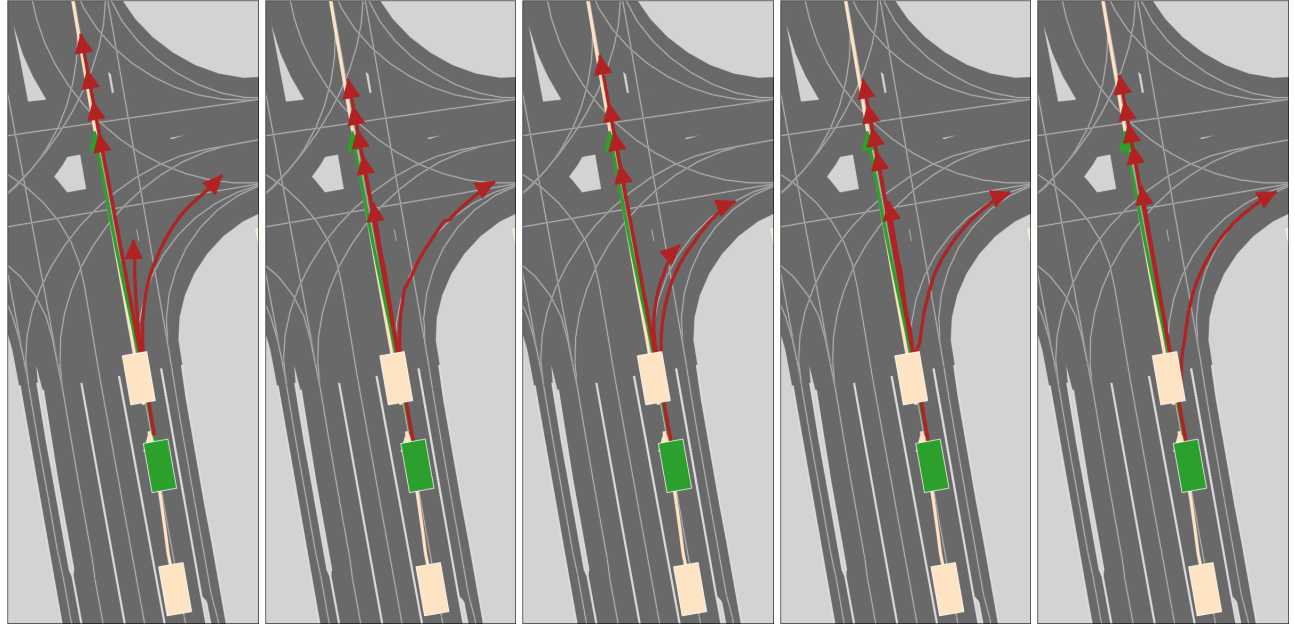
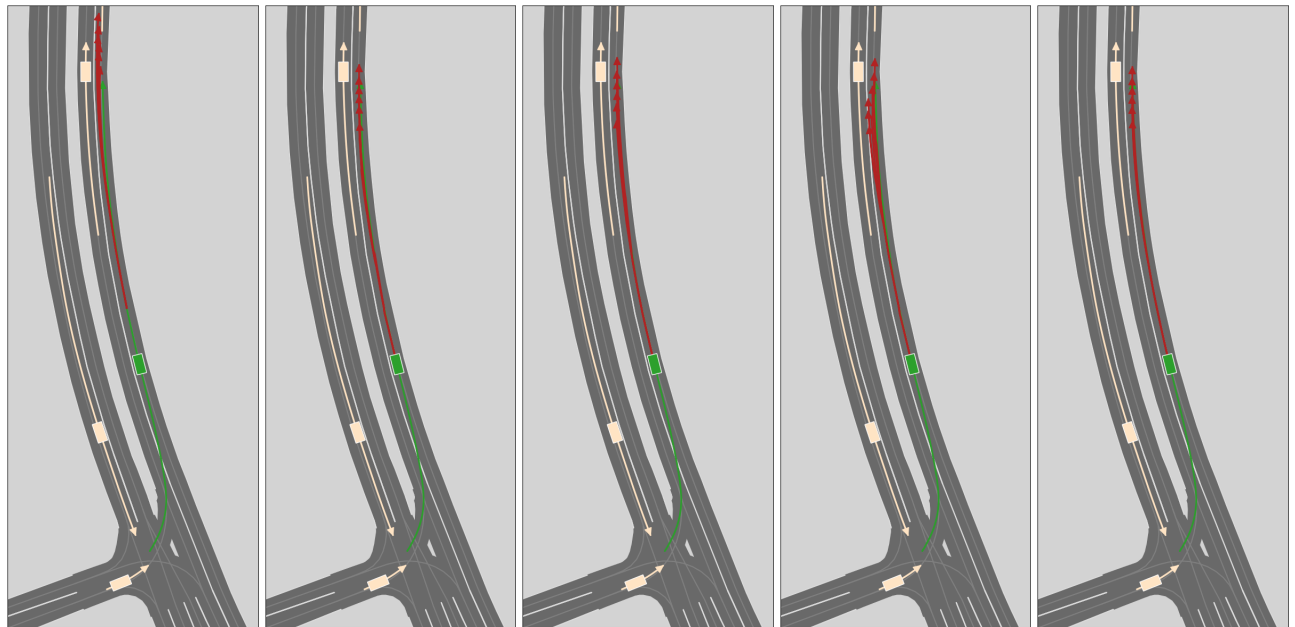


Figure 7. Failure cases of DONUT.



(a) Encoder-decoder (b) DONUT Overp. ✗ Ref. ✗ (c) DONUT Overp. ✓ Ref. ✗ (d) DONUT Overp. ✗ Ref. ✓ (e) DONUT Overp. ✓ Ref. ✓

Figure 8. Additional qualitative results.



(a) Encoder-decoder (b) DONUT Overp. ✗ Ref. ✗ (c) DONUT Overp. ✓ Ref. ✗ (d) DONUT Overp. ✗ Ref. ✓ (e) DONUT Overp. ✓ Ref. ✓

Figure 9. Additional qualitative results.

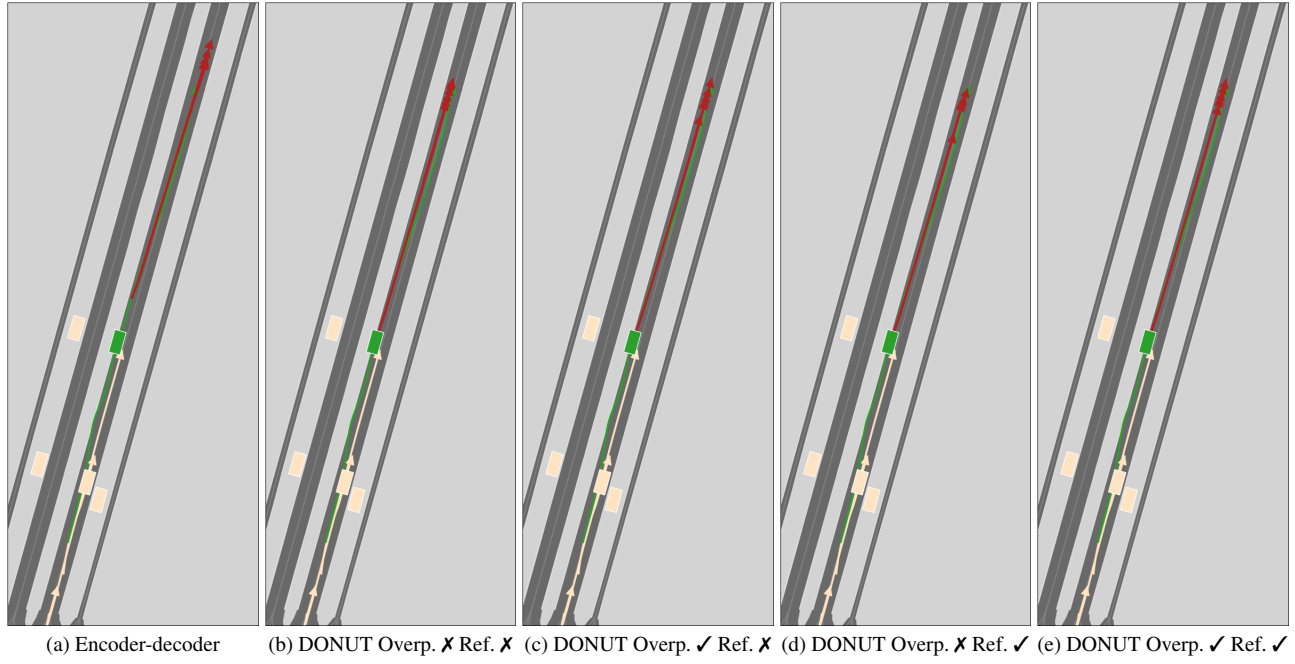


Figure 10. **Additional qualitative results.**

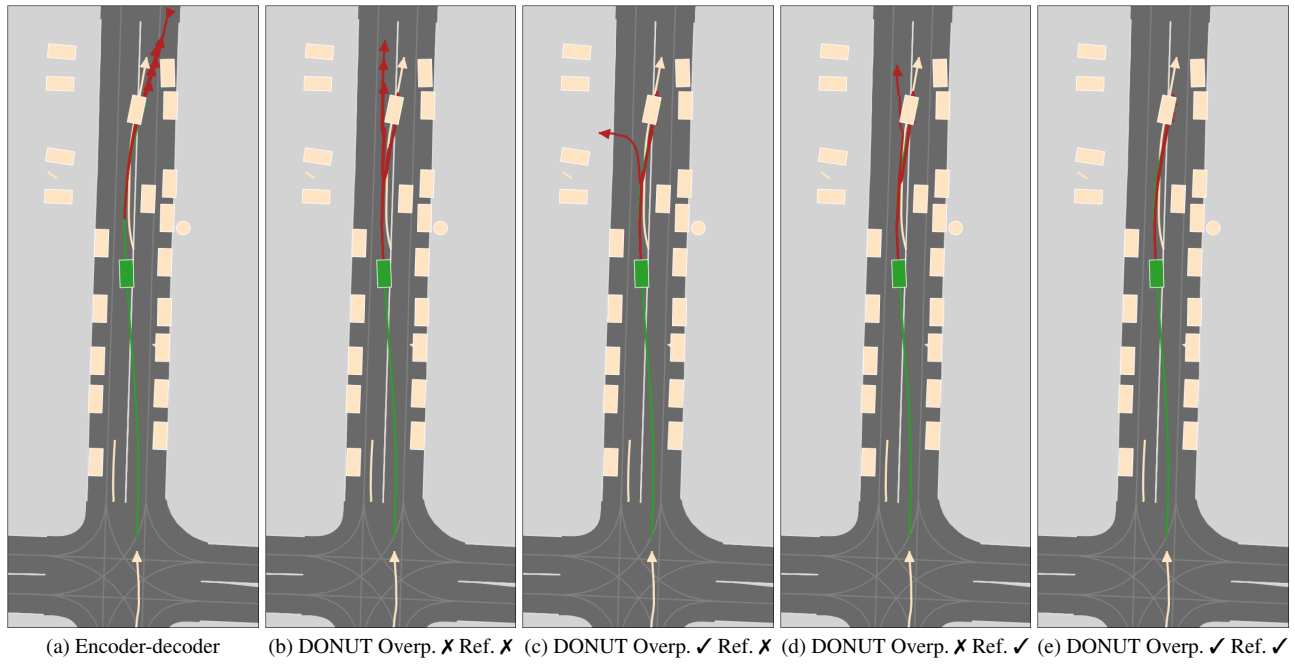
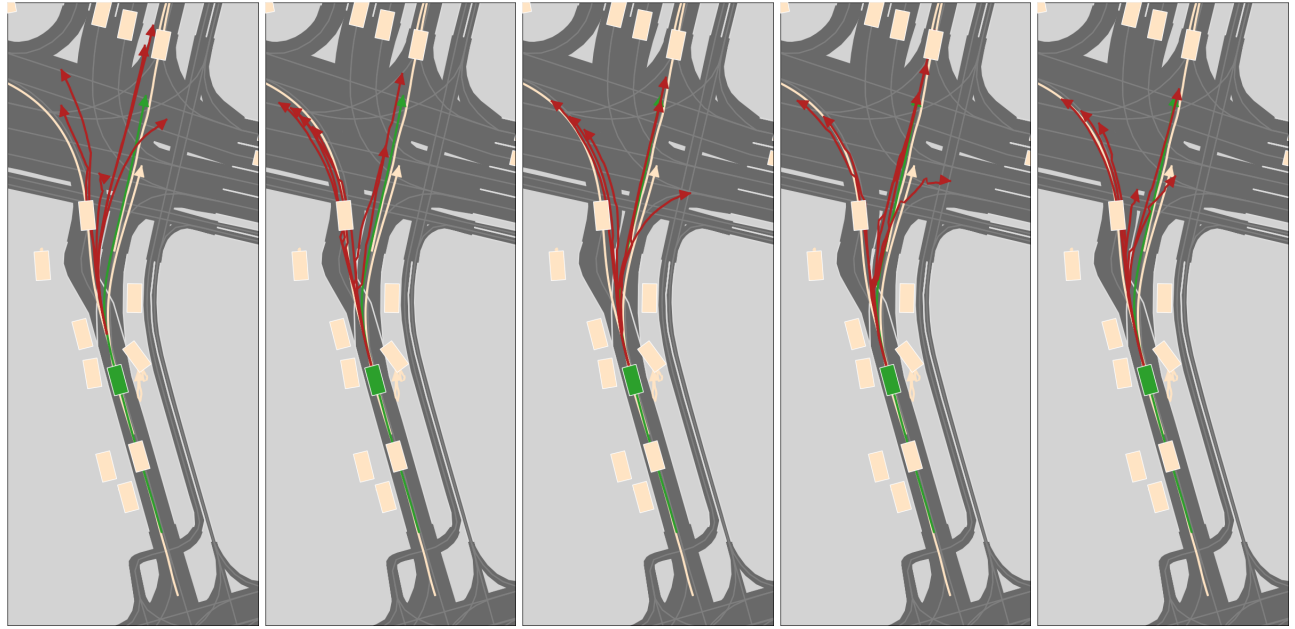
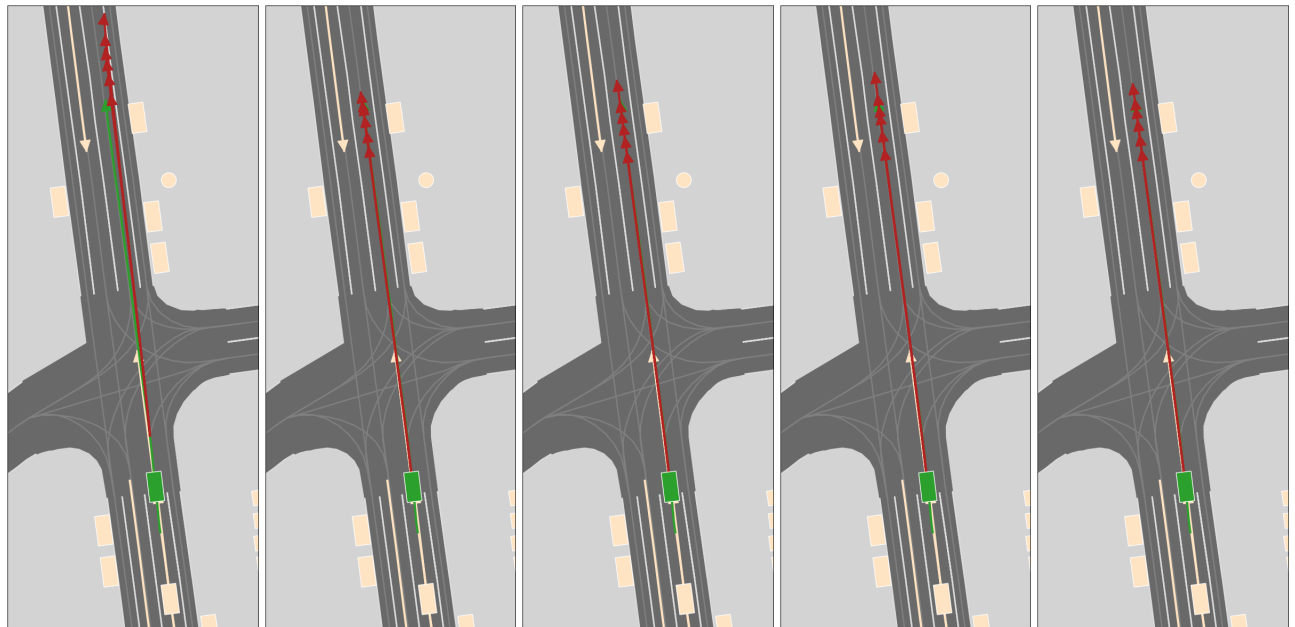


Figure 11. **Additional qualitative results.**



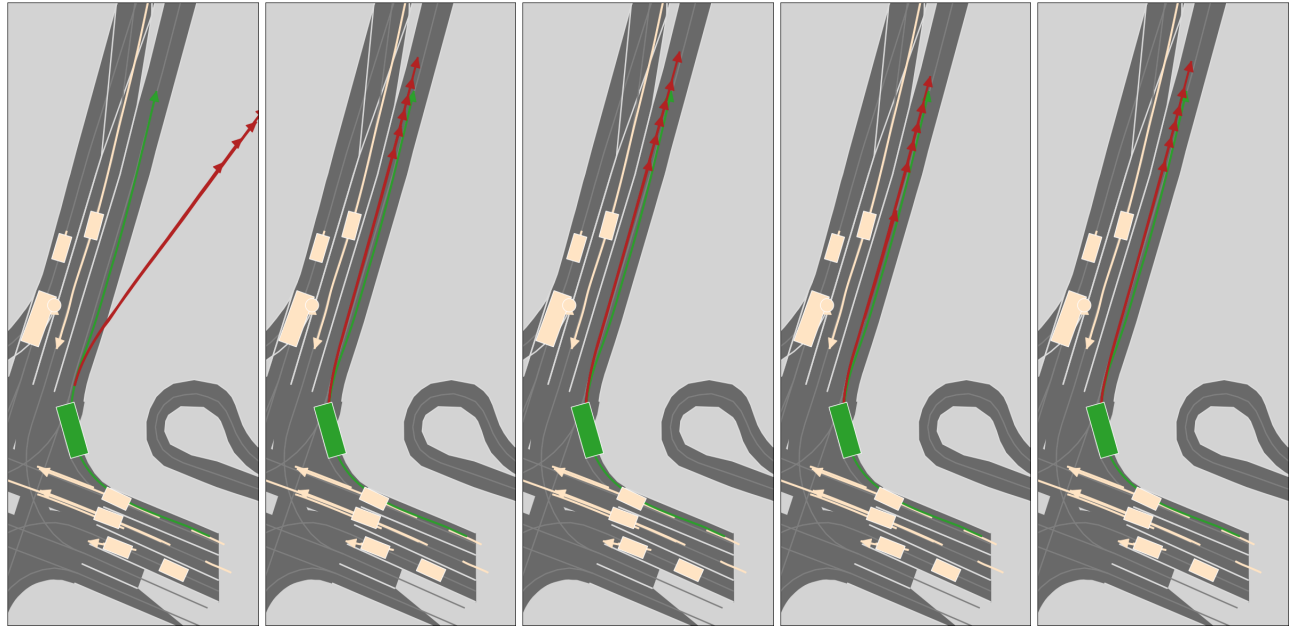
(a) Encoder-decoder (b) DONUT Overp. ✗ Ref. ✗ (c) DONUT Overp. ✓ Ref. ✗ (d) DONUT Overp. ✗ Ref. ✓ (e) DONUT Overp. ✓ Ref. ✓

Figure 12. Additional qualitative results.



(a) Encoder-decoder (b) DONUT Overp. ✗ Ref. ✗ (c) DONUT Overp. ✓ Ref. ✗ (d) DONUT Overp. ✗ Ref. ✓ (e) DONUT Overp. ✓ Ref. ✓

Figure 13. Additional qualitative results.



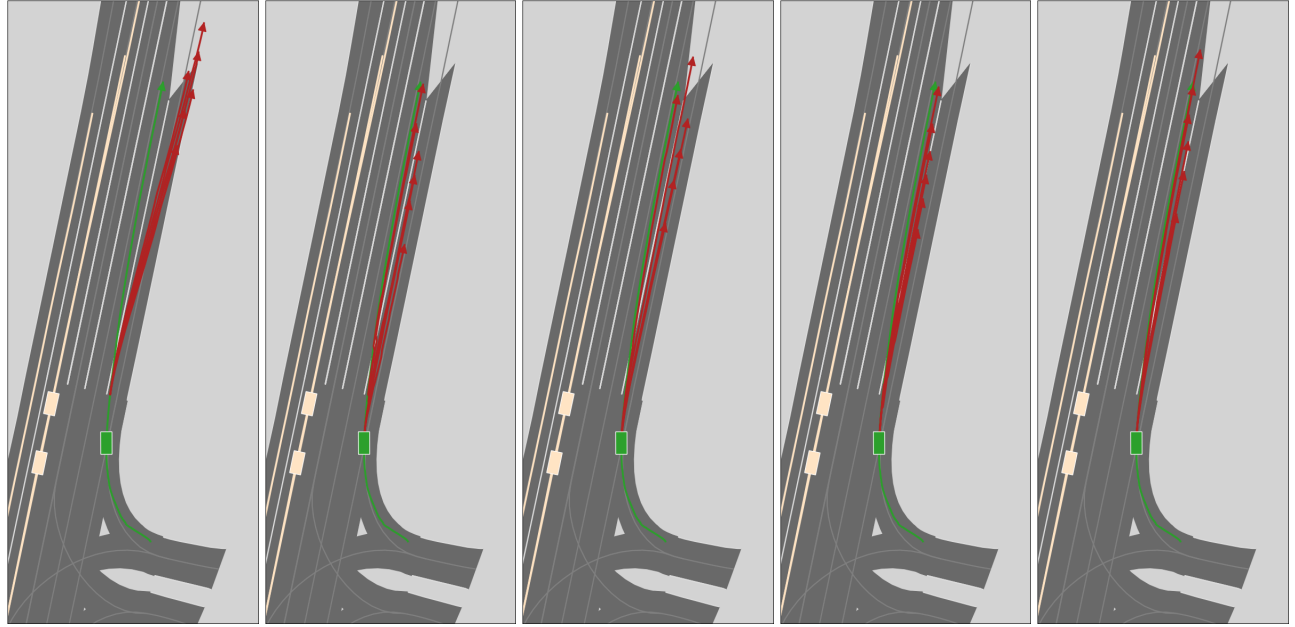
(a) Encoder-decoder (b) DONUT Overp. ✗ Ref. ✗ (c) DONUT Overp. ✓ Ref. ✗ (d) DONUT Overp. ✗ Ref. ✓ (e) DONUT Overp. ✓ Ref. ✓

Figure 14. Additional qualitative results.



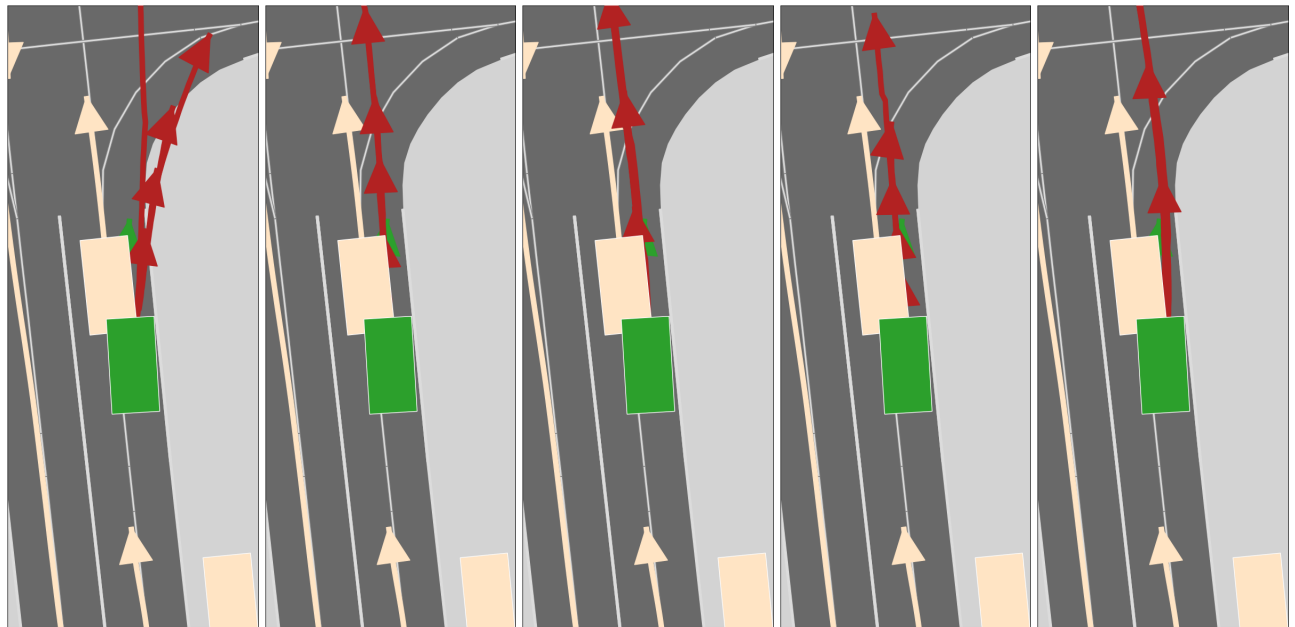
(a) Encoder-decoder (b) DONUT Overp. ✗ Ref. ✗ (c) DONUT Overp. ✓ Ref. ✗ (d) DONUT Overp. ✗ Ref. ✓ (e) DONUT Overp. ✓ Ref. ✓

Figure 15. Additional qualitative results.



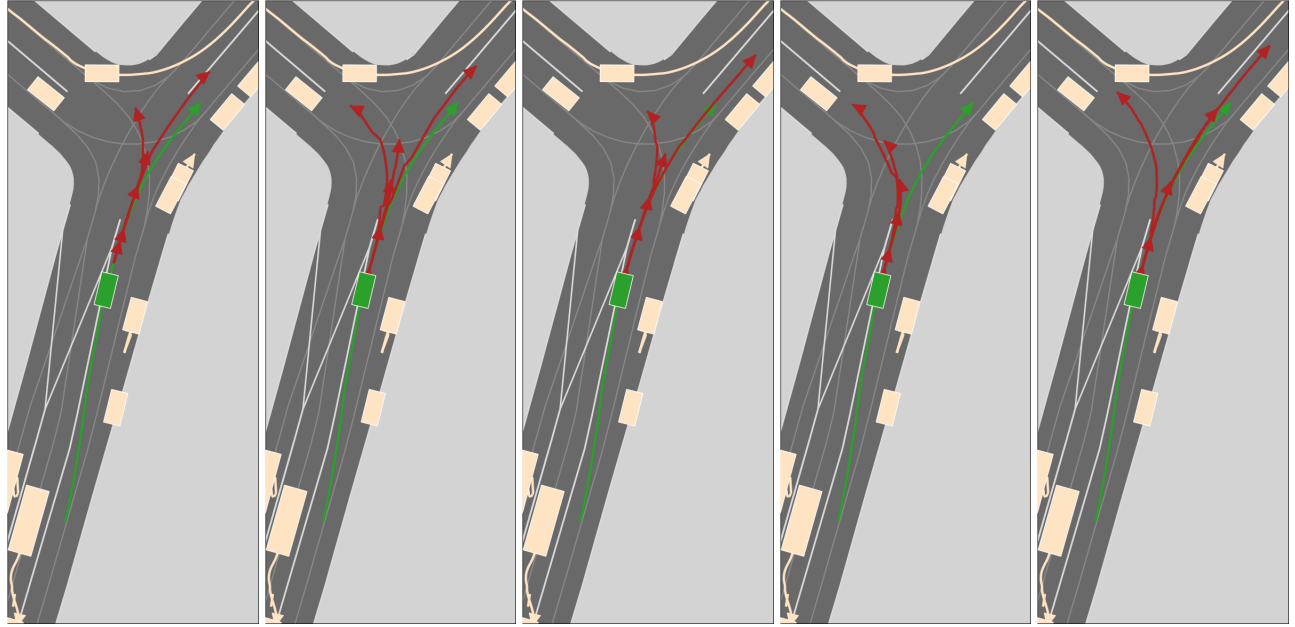
(a) Encoder-decoder (b) DONUT Overp. ✗ Ref. ✗ (c) DONUT Overp. ✓ Ref. ✗ (d) DONUT Overp. ✗ Ref. ✓ (e) DONUT Overp. ✓ Ref. ✓

Figure 16. Additional qualitative results.



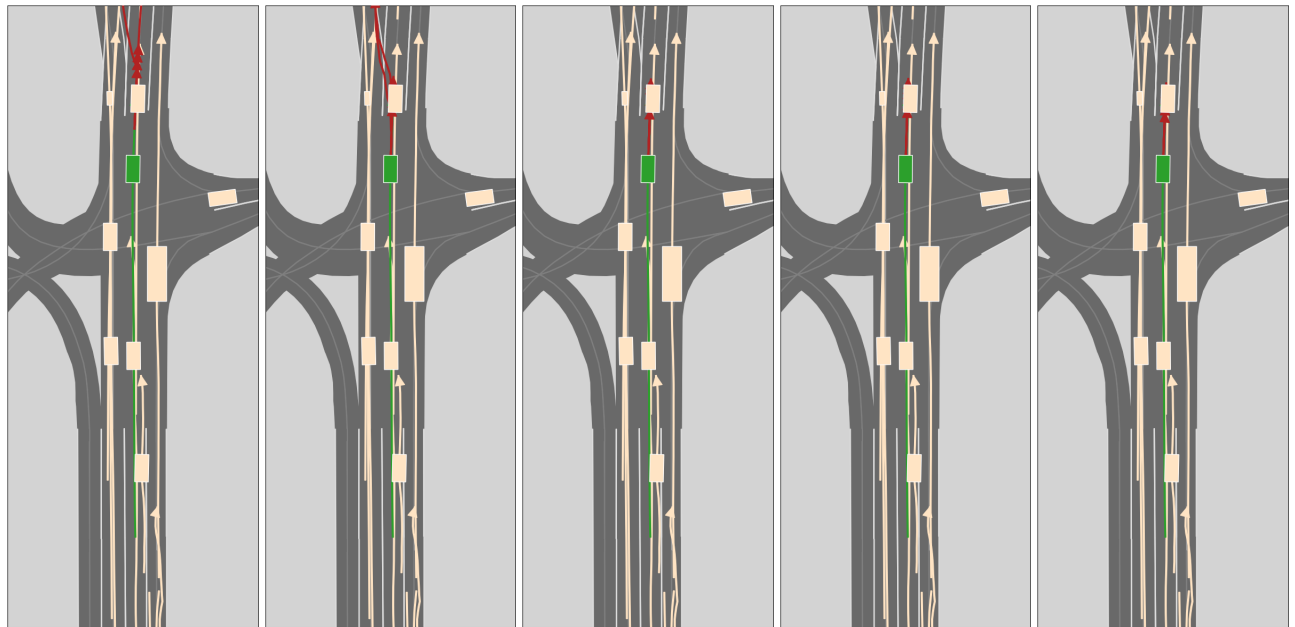
(a) Encoder-decoder (b) DONUT Overp. ✗ Ref. ✗ (c) DONUT Overp. ✓ Ref. ✗ (d) DONUT Overp. ✗ Ref. ✓ (e) DONUT Overp. ✓ Ref. ✓

Figure 17. Additional qualitative results.



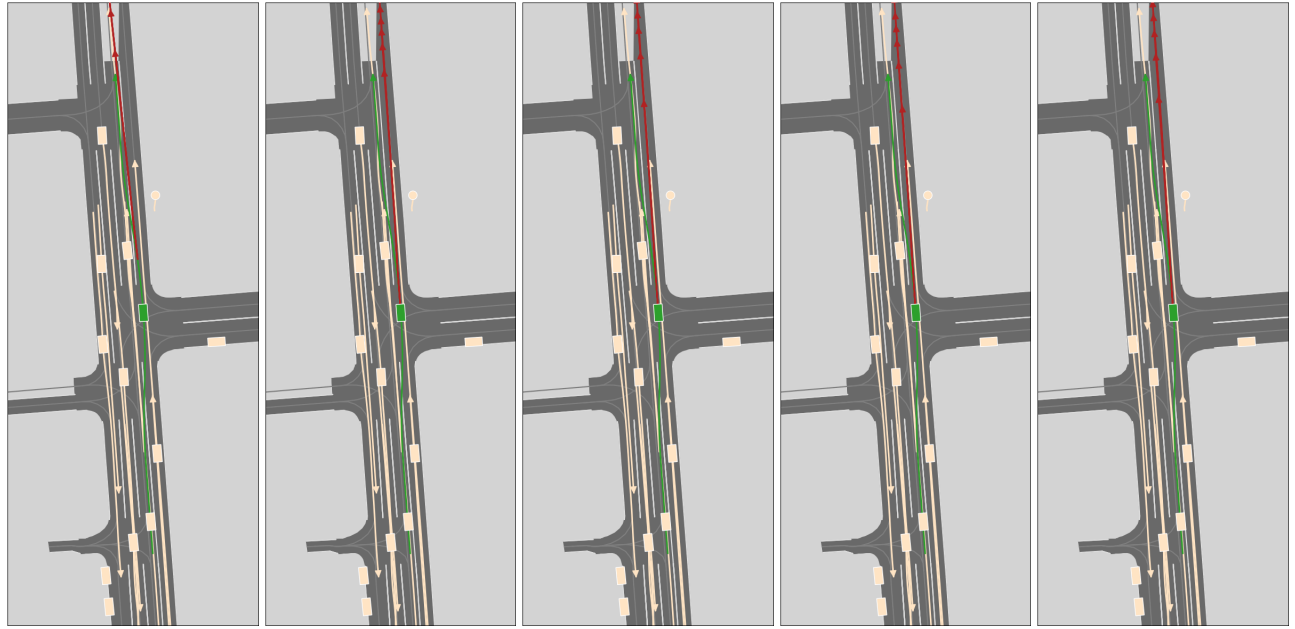
(a) Encoder-decoder (b) DONUT Overp. ✗ Ref. ✗ (c) DONUT Overp. ✓ Ref. ✗ (d) DONUT Overp. ✗ Ref. ✓ (e) DONUT Overp. ✓ Ref. ✓

Figure 18. Additional qualitative results.



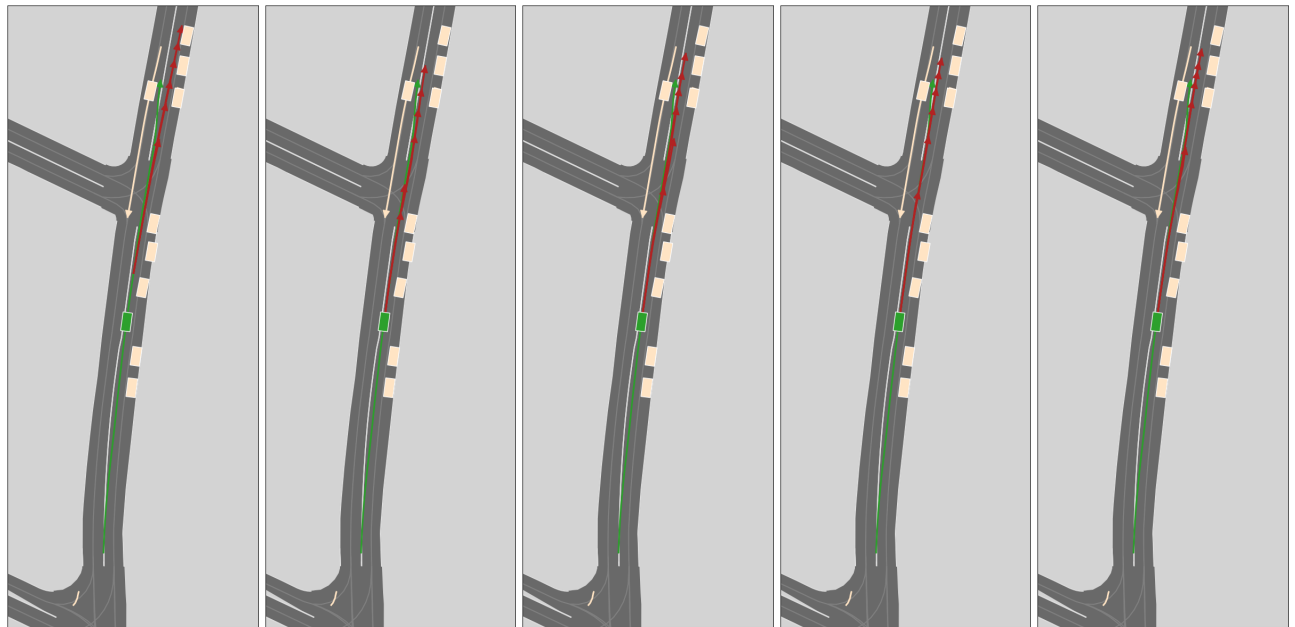
(a) Encoder-decoder (b) DONUT Overp. ✗ Ref. ✗ (c) DONUT Overp. ✓ Ref. ✗ (d) DONUT Overp. ✗ Ref. ✓ (e) DONUT Overp. ✓ Ref. ✓

Figure 19. Additional qualitative results.



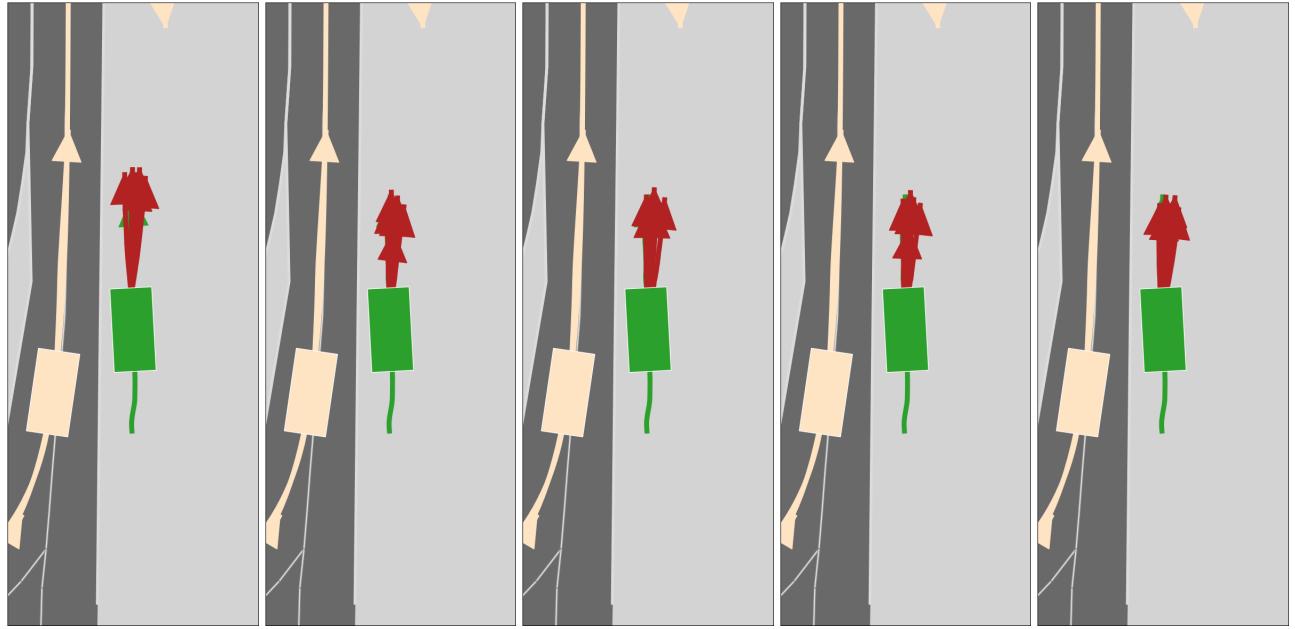
(a) Encoder-decoder (b) DONUT Overp. ✗ Ref. ✗ (c) DONUT Overp. ✓ Ref. ✗ (d) DONUT Overp. ✗ Ref. ✓ (e) DONUT Overp. ✓ Ref. ✓

Figure 20. Additional qualitative results.



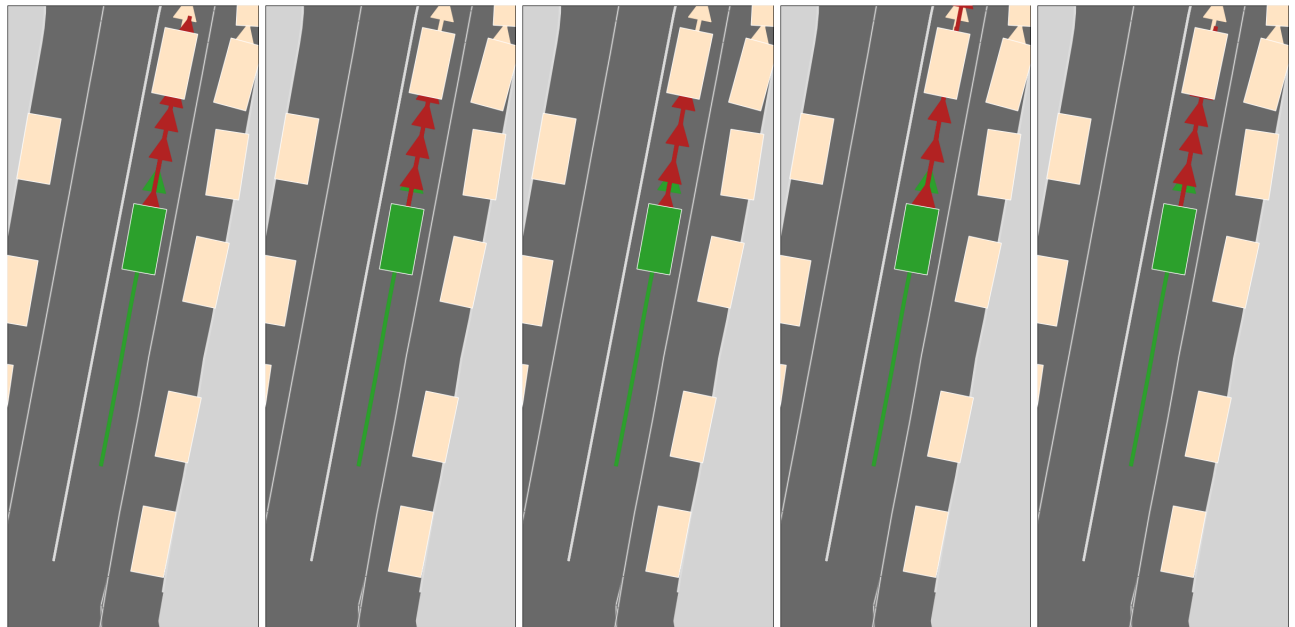
(a) Encoder-decoder (b) DONUT Overp. ✗ Ref. ✗ (c) DONUT Overp. ✓ Ref. ✗ (d) DONUT Overp. ✗ Ref. ✓ (e) DONUT Overp. ✓ Ref. ✓

Figure 21. Additional qualitative results.



(a) Encoder-decoder (b) DONUT Overp. ✗ Ref. ✗ (c) DONUT Overp. ✓ Ref. ✗ (d) DONUT Overp. ✗ Ref. ✓ (e) DONUT Overp. ✓ Ref. ✓

Figure 22. Additional qualitative results.



(a) Encoder-decoder (b) DONUT Overp. ✗ Ref. ✗ (c) DONUT Overp. ✓ Ref. ✗ (d) DONUT Overp. ✗ Ref. ✓ (e) DONUT Overp. ✓ Ref. ✓

Figure 23. Additional qualitative results.